Review

Ahmed Ali*, Hassan Barada and Moh'd Rezeq

Characterization and modeling of nanotips fabricated in the field ion microscope

DOI 10.1515/ntrev-2015-0037
Received July 16, 2015; accepted October 16, 2015; previously published online June 2, 2016

Abstract: Nanotips are considered significant elements in some of nanotechnology instruments. They are used in scanning probe microscopes and electron microscopes to characterize materials at the nano and atomic scales. Therefore, the size and profile of the nanotip determines the performance of these microscopes. The advancement of nanotip fabrication techniques has enabled the fabrication of ultra-sharp tips and even single-atom tips. However, the characterization of nanotips with an apex of a few nanometers is still premature, while the conventional characterization methods of the tip size, such as the ring counting method, have shown some limitation at this nano scale. In this paper, we review the various nanotip fabrication methods with a focus on the most recent one, which is called the local electron bombardment method. We demonstrate an approach for estimating the nanotip radius with good approximation using ball crystal models. We also model the overall nanotip profile using finite element simulation tools based on the hyperboloidal geometry. The modeling and radius estimation approach is applied on tips fabricated by the local electron bombardment method, which will be explained in detail as well.

Keywords: characterization; fabrication; modeling; nanotips; simulation.

***Corresponding author: Ahmed Ali,** Department of Electrical and Computer Engineering, Khalifa University of Science, Technology and Research, Abu Dhabi, United Arab Emirates,
e-mail: ahmed.ali@kustar.ac.ae
Hassan Barada: Department of Electrical and Computer Engineering, Khalifa University of Science, Technology and Research, Abu Dhabi, United Arab Emirates
Moh'd Rezeq: Department of Electrical and Computer Engineering, Khalifa University of Science, Technology and Research, Abu Dhabi, United Arab Emirates; and Department of Applied Mathematics and Sciences, Khalifa University of Science, Technology and Research, Abu Dhabi, United Arab Emirates

1 Introduction

The invention of the field ion microscope (FIM) >65 years ago had allowed characterization of sharp tips with atomic resolution [1]. In FIM, the sample, which is a sharp tip, is placed inside an ultra-high vacuum (UHV) chamber in front of a phosphor screen. The tip is positively biased with a high voltage in the presence of an inert gas, like helium, inside the chamber. When the applied electric field reaches the ionization threshold (e.g. ≈5 V/Å when helium gas is used in the chamber), the gas atoms get polarized and then attracted to the tip apex. As the polarized atom settles on the apex surface, it gets ionized by losing an electron as it tunnels to the apex surface. Consequently, the positive ion is instantly repelled from the surface and then follows the field trajectory toward the screen. The position where the ions hit the screen accurately represents the atomic sites on the tip apex. A micro-channel plate (MCP), which is attached to the screen, intensifies the image brightness. Consequently, the produced FIM image can show the atomic structure of the tip apex [2–4]. The field emission microscope (FEM), which was developed earlier than the FIM, has a similar setup. However, the tip here is negatively biased and no gases exist inside the UHV chamber. Electrons will be emitted through a quantum tunneling process when the applied field reaches a value around 5 V/nm [5]. They follow the field trajectory where they eventually hit the screen. The electron emission current density varies according to the local work function of the tip surface atomic planes. Therefore, the resulting FEM image shows bright and dark zones. Figure 1 shows a schematic of an FEM [6, 7]. Due to the random lateral movement of the emitted electrons and the non-localized electron density, it is not possible to achieve atomic resolution with FEM.

1.1 Nanotip fabrication techniques

The importance of fabricating ultra-sharp tips with a good profile for various applications in nanotechnology has been the main motivation to develop reliable nanotip

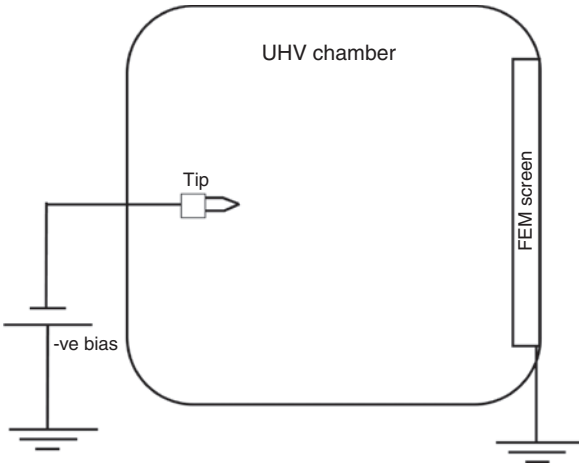

Figure 1: Schematic of an FEM.

fabrication techniques. Several notable methods have been introduced. They are summarized in the following subsections.

1.1.1 Field surface melting and build-up

In this method, a high electric field (around 2.55 V/Å in case of tungsten tip) is applied on the tip, which reduces the activation energy of the surface atoms. Then, the tip is heated to a temperature that is a third of the bulk melting temperature. The atoms will then diffuse and build up on the tip apex where the electric field is enhanced. The formed nanotip here can be used as an atomic metallic ion emission source by controlling the tip temperature and the applied electric field. This will ensure continuous surface melting so that the atoms keep diffusing toward the apex where they successively get ionized. As a result, a continuous ion beam is emitted from the topmost end of the nanotip [8–12].

1.1.2 Atom deposition on tips sharpened by ion sputtering

The tip here is first sharpened by ion sputtering, which leads to the removal of the tip surface atoms. The sharpening continues until the formation of a stable trimmer apex. After that, a metal atom is deposited on the trimmer apex using a metal evaporator [13].

1.1.3 Tip coating with certain metals such as palladium

In this method, a (111) oriented tip is coated with a noble metal such as palladium where it gets adsorbed on the tip surface. This will induce anisotropy of the surface energy in the (111) plane. In this case, annealing the tip will cause surface atoms to diffuse and form pyramidal protrusion in order to settle in a low surface energy state [14–17]. The nanotips prepared with this method are thermally stable and easy to reproduce, as the reproduction requires only tip annealing [18–23].

1.1.4 Controlled field-assisted gas etching

In this method, an etchant gas such as nitrogen is introduced in a UHV chamber while the tip is positively biased. The electric field on the tip apex is normally higher than on its shank. By taking advantage of this fact, the applied voltage on the tip can be adjusted such that the electric field on the apex is higher than the evaporation threshold of the nitrogen gas. Therefore, it will be confined to the tip shank surrounding. The nitrogen gas will dissociate and get adsorbed on the tip shank, causing the tip atoms to protrude out of their places. This protrusion will cause the electric field to enhance locally and exceed the evaporation threshold of the tip material, and leads to the tip atoms being evaporated locally. This process will continue to occur exclusively on the shank, and leads to the tip getting sharper, resulting in a single-atom tip (SAT) [24–27].

1.1.5 Local electron bombardment

This most recent method utilizes electrons emitted from a hot metal ring surrounding the tip to locally bombard the tip shank. The ring is made from one of the following refractory metals: tungsten, niobium, molybdenum, tantalum, rhenium, osmium, and iridium. In addition, the ring can be composed of an alloy of two or more of these mentioned metals. The ring diameter is about 2–4 mm. It is placed around the tip shank below the tip end and connected to a DC current source. The ring should be placed at least 1 mm below the tip that is connected to a positive DC high-voltage source. The electrons are extracted from the ring and accelerated along the electric field to hit the tip shank with high kinetic energy, causing atoms to be displaced from their position. Subsequently, these atoms will diffuse toward the tip apex where they either evaporate due to the apex high field or stay on the apex forming a pyramid-like or conical protrusion, thus increasing the tip aspect ratio. This method's setup is schematically illustrated in Figure 2. The dashed lines represent the trajectory of the electrons emitted from the hot ring, whereas the solid lines represent the field lines directed toward the MCP [28].

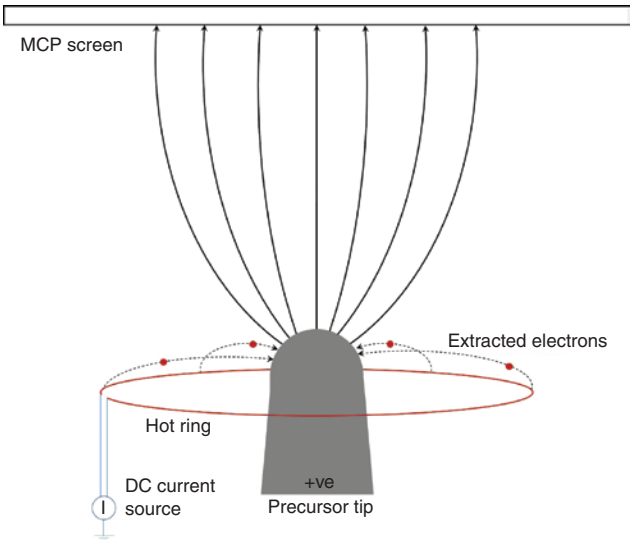

Figure 2: Schematic for the local electron bombardment setup.

Local electron bombardment has several advantages over the previous methods:

1. The method does not depend on certain surface or crystal properties of the tip material. Therefore, it can be used with any tip consisting of metals or heavily doped semiconductors. Also, it can be used with materials of any crystal orientation, polycrystalline materials, or even amorphous materials.
2. The process only involves controlled bombardment of the tip with electrons. No gases or foreign materials are involved in the fabrication process, and thus it can be considered as a clean method.
3. The method can be performed blindly, i.e. without the need for FIM. This will simplify the tip restoration process and any unnecessary contamination resulting from transferring the tip to the FIM is avoided.
4. The method allows the sharpening process to be performed while monitoring its progress in FIM. This allows good control on the shape of the produced tip. The supply of the imaging gas is slightly reduced in order to avoid its interference with the electrons that are bombarding the tip.
5. The atom diffusion toward the tip apex during the fabrication process will increase the tip aspect ratio, which is an advantage for any fabricated tip.

2 Experimental procedure and results

The initial tip is fabricated from a clean tungsten wire with a radius of 0.25 mm. As the local electron bombardment can work with any crystal orientation, the tungsten wire used here is polycrystalline, which is considered inexpensive compared to single crystal wires. The wire is initially sharpened using AC chemical etching method by placing it in a thin film of KOH solution [29–33]. The tip resulting from this process is typically in the range of 10–50 nm, which is good enough for the FIM imaging process with an applied tip voltage around 5–30 kV. The initial tip is then transferred to the FIM UHV chamber for further cleaning. The tip is annealed (at around 1500–1800 K) for 15–20 min to remove any contaminations and oxide layers. Then, the tip is set for the field evaporation process in FIM where it can be cleaned from any roughness or defects until a smooth tip apex surface is obtained. For performing this process, an inert gas such as helium is introduced into the chamber to serve as an imaging gas. The voltage is increased gradually so that the electric field produced by the tip reaches the imaging field where the tip atomic structure appears on the screen. Then, we increase the tip voltage gradually to remove any protrusions or defects, by field evaporating the tip atoms until a clean and smooth tip apex is obtained.

At this stage, the tip is ready for the sharpening process, and the applied voltage is reduced slightly to maintain the field at the threshold FIM imaging value. The ring around the tip is then connected to a current source. The current is carefully increased while monitoring the ring color until reaching a temperature to cause a Schottky field emission (1800–2000 K). During the sharpening process and as the tip gets sharper, the electric field produced by the tip increases. As a result, the applied voltage is gradually decreased to maintain the threshold electric field at the imaging value in order to avoid evaporation of atoms from the center of the apex. Moreover, the current passing through the metal ring can also be adjusted in order to control the ring temperature, and hence the extracted electrons. This will help in optimizing the sharpening process.

Figure 3 shows a sequence of FIM images while using the local electron bombardment method to fabricate a SAT. The process starts with an initial clean tip of around 16 nm, as estimated from Figure 3A using the ring counting method [1]. Moreover, the tip apex structure indicates that it is slightly tilted from the (110) orientation. However, the planes can be recognized using the standard stereographic projection maps of the bcc structure [1]. During the fabrication process, the ring current is set to 1.4 A. This results in heating the ring to a temperature of about 1800 K. Also, helium gas is introduced in the chamber at a pressure of 10^{-5} Torr. The initial tip, which is shown in Figure 3A, was imaged at around 8.3 kV. The subsequent

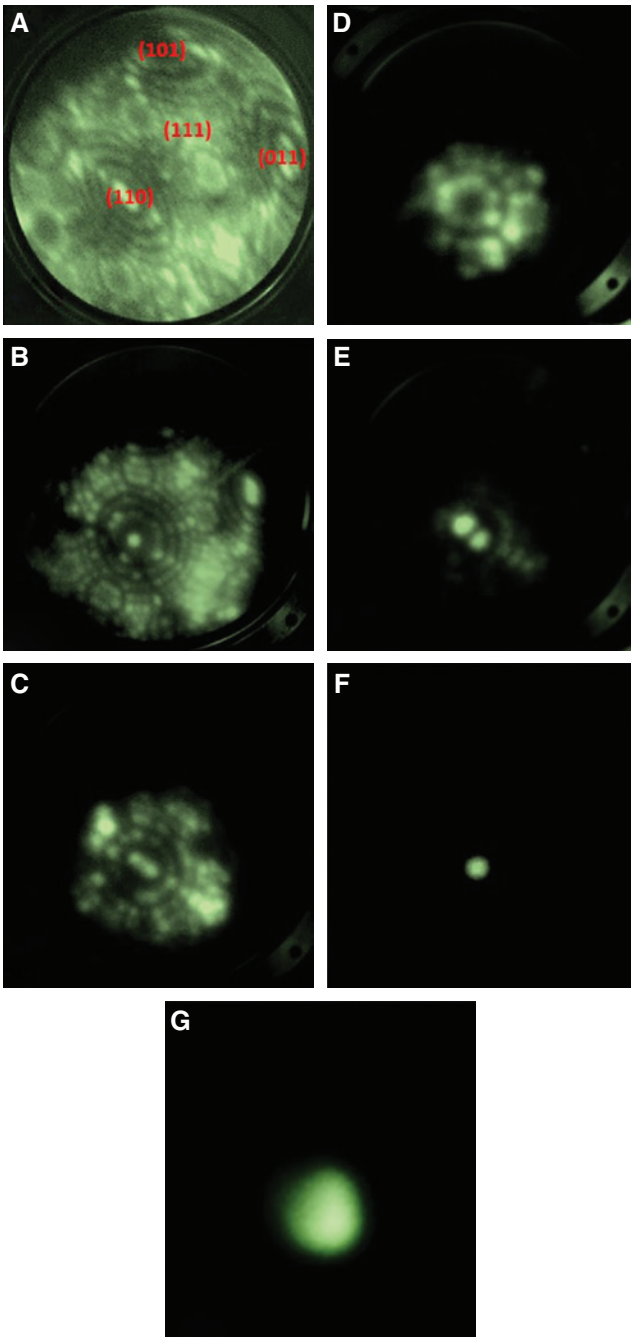

Figure 3: FIM image sequence showing the sharpening process on the tip apex. (A) The initial tip. (B–E) Intermediate stages of the tip during the sharpening process. (F) The SAT formation on the tip. (G) FEM image of the SAT shown in (F).

images (B–E) in Figure 3 are imaged at 6.4, 5.0, 4.1, and 3.6 kV, respectively. The image sequence shows that the tip apex gets smaller over time until reaching a single-atom apex (as shown in Figure 3F). The SAT is imaged at 2.5 kV. It can be realized from the image sequence in Figure 3 that the apex size gets smaller and the atoms are magnified, which indicate the tip sharpening. Another indication of the tip sharpness is the continuous reduction of the voltage required for imaging of the tip apex. The SAT shown in Figure 3F was also tested in field emission mode. This resulted in a bright and confined electron beam, as shown in Figure 3G. The field emission shown in this figure was obtained at -300 V.

3 Nanotip modeling and radius estimation

Modeling the atomic structure of the nanotip is a useful way to estimate the tip shape and size [34–36]. The three-dimensional ball model is generated by building a bcc cubical structure knowing the atom size and the lattice constant of tungsten. Then, a spherical cut is taken from this structure with an appropriate radius in a way to reasonably reproduce the apex surface atomic structure.

Figure 4A and B show two FIM images with different sizes. Figure 4A was imaged at 4.8 kV, whereas Figure 4 was imaged at 5.4 kV. The ball model to the right of each image, namely Figure 4C and D, represents the corresponding FIM images by locating most of the surface atoms on the apex with the same number of steps (rings) and atomic configuration. It can be realized from the FIM images in Figure 4 that not all the atoms in the spherical model appear in the FIM image. This is because the overall shape of the tip follows a hyperboloidal geometry rather than a spherical geometry. Figure 4E schematically illustrates the hyperbolic shape of the apex. The apex part, which is labeled in blue, only represents the FIM image. The dashed part in the figure does not exist in the FIM image. The electric field on the shank is below the imaging field threshold. Therefore, the shank, which represents the dark region around the FIM image, does not show. In addition, in such small tips, some atoms from the apex surface may evaporate due to the local field enhancement that exceeds the imaging field and reaches the evaporation field threshold. Some other atoms can get dislocated from their regular position due to the field stress. As a result, very few atoms are either added or removed from their lattice position to match the FIM atomic image. There are also some atoms displaced from their lattice positions due to the high electric field on the apex.

Modeling the tip atomic structure (as illustrated in Figure 4 as an example) will provide a more accurate method to estimate the tip radius for relatively small tips. For broad tips, >5 nm radius, the size of the tip apex is usually estimated using the “ring counting method,” as we describe briefly here [1]. This method utilizes the

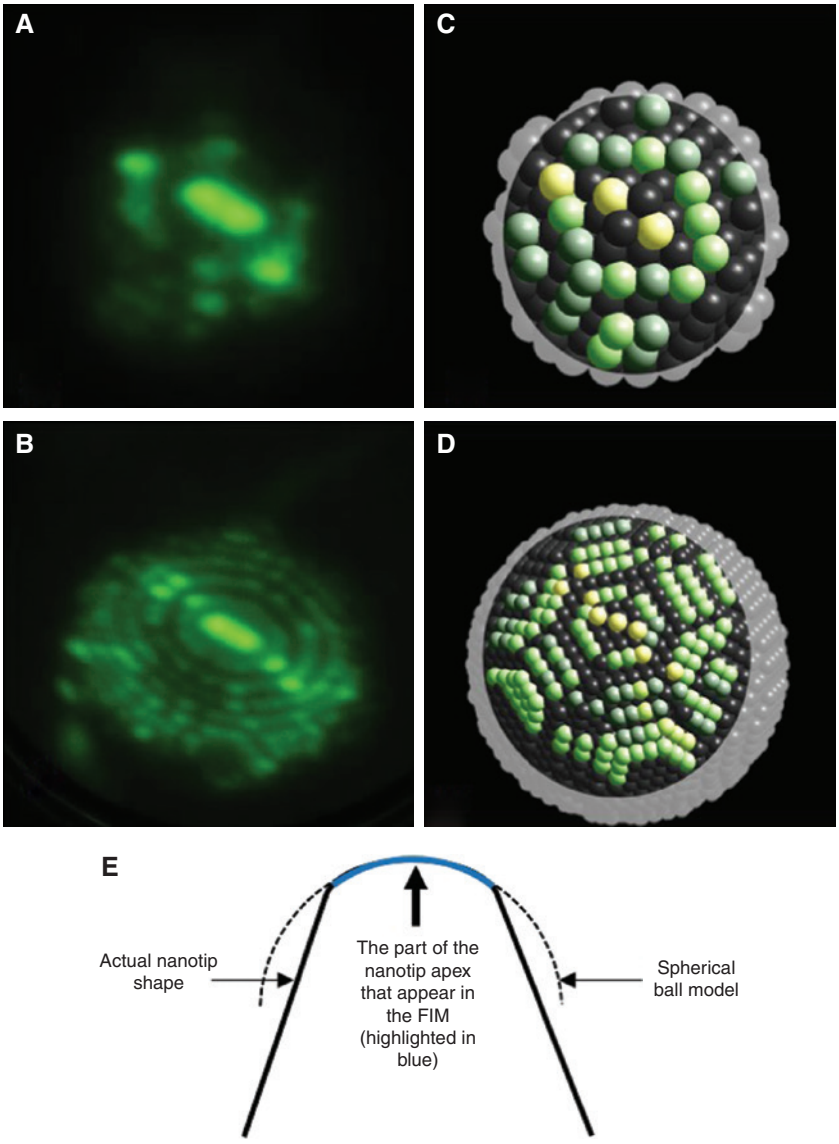

Figure 4: FIM images for (A) a nanotip with a radius of 1.18 nm and (B) a nanotip with a radius of 3.02 nm. Ball model representation for (C) the nanotip in A and (D) the nanotip in B. (E) A schematic showing the lateral view of a nanotip.

angular separation (θ) between two identified poles of selected atomic planes to obtain the radius of curvature of the nanotip apex (R). Figure 5A illustrates this method by showing a lateral view of a tip apex with planes (hkl) and ($h'k'l'$) separated by θ. Due to the crystallographic nature of the tip structure (bcc in this example), the tip apex will show a number of atomic steps (n) when moving from (hkl) to ($h'k'l'$) plane, as shown in Figure 5A. The atomic layers (steps) are separated by a spacing (s), which is given by the following equation for cubic crystals:

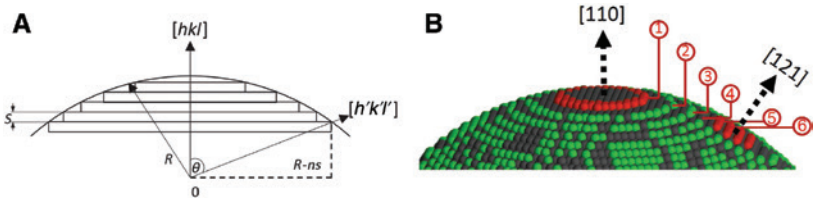

Figure 5: (A) A schematic showing a lateral view of a tip. (B) A ball model with a radius of 10 nm corresponding to the schematic in A.

$$s=\frac{a}{\delta\sqrt{h^2+k^2+l^2}}, \quad (1)$$

where a is the crystal lattice constant and δ is a constant depending on the three miller indices h, k, and l. For the bcc crystal structure, δ is 1 if $h+k+l$ gives an even number, while δ is 2 if $h+k+l$ gives an odd number. The radius R can then be computed from the dashed triangle in Figure 5A as

$$R=\frac{ns}{1\text{-}\cos\theta}. \quad (2)$$

The atomic steps represent the edges of atomic planes on the apex crystal structure; as a result, they will have a relatively higher electric field than other atoms within the same plane. Those edge atoms will consequently appear brighter and form round rings in the FIM image, which can be used as a guidance to count the number of steps between the planes. A model of a tip with a radius of 10 nm is shown in Figure 5A as an example of applying the ring counting method to estimate the tip radius. The (110) plane and (121) plane are selected here to calculate the radius of curvature. Those planes are highlighted in red. The figure shows that there are six steps from the (110) plane to the center of the (121) plane. By substituting the number of steps in Eq. (2), we get a radius of 9.6 nm, which shows an around 4% difference from the actual radius of the model.

The ring counting method can be applied with a reasonable accuracy for relatively large tips. As the tip gets smaller, the percentage error resulting from applying this method increases. For example, if we apply the ring counting method on the ball model in Figure 4D (which is shown again in Figure 6), we count 7.5 steps from the (110) plane to the center of the (011) plane. Substituting the number of steps in Eq. (2) gives a radius of 3.35 nm. Comparing this value with the radius of the model in Figure 4B, we see a difference of around 11%. Also, as the tip gets smaller, it shows less number of planes, which limits the selection of the best planes for accurate application of the ring counting method. Furthermore, for tips <3 nm, we can only recognize the top atomic plane. It is clear that if an accurate estimate of the tip radius is needed, especially for relatively small tips (<5 nm), modeling the tip atomic structure (as illustrated in Figure 4) has to be performed.

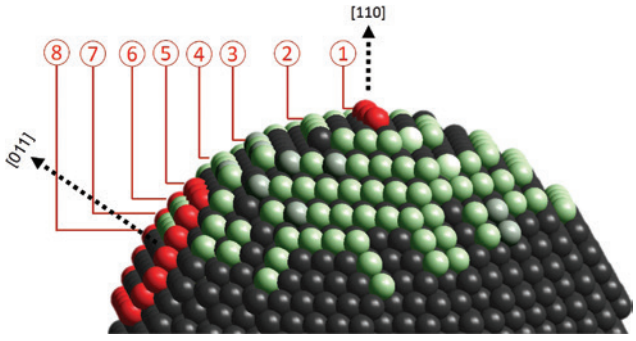

Figure 6: Illustration of the use of ring counting method on the same ball model shown in Figure 4D.

4 Finite element simulation of the nanotip profile

Tip radius estimation is used to determine the tip's sharpness. However, this provides an estimation of the apex size only but gives no information about the tip profile. The base size is significantly important because it affects the value of the electric field generated by the tip at a certain applied voltage. A nanotip with a large base cannot generate the electric field expected from such nanotip size at the same applied voltage [7, 37].

Finite element simulation (FES) is useful here to characterize the overall tip profile [38]. As indicated in Figure 4, the tip's overall shape follows a hyperboloidal geometry. Therefore, we select the elliptic coordinate system to draw our FES model. Figure 7 shows a schematic of the FES model where the tip base (u_o) and the nanotip are drawn according to the hyperbolic profile. Another hyperbolic profile (u) is drawn 200 nm away from the tip to represent a boundary condition, which is needed for meshing purposes.

The profiles are drawn according to the following equations of the elliptic coordinate system [39]:

$$z=L\cos(u)\cosh(v), \quad (3)$$

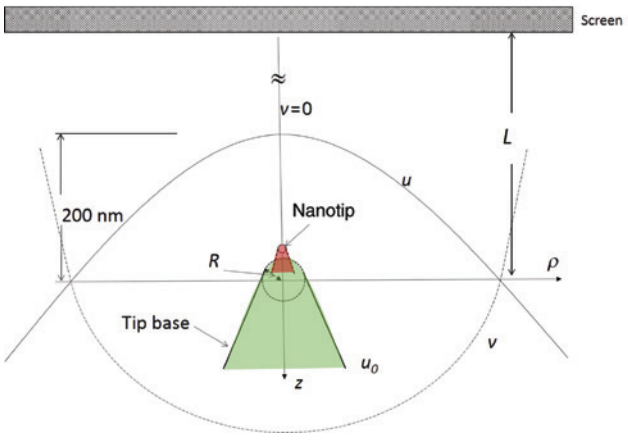

Figure 7: A schematic of the FES model of a nanotip.

$$\rho = L\sin(u)\sinh(v), \tag{4}$$

where L is the distance between the center of the tip base and the screen. To find u_o, we set $\rho=0$ in Eq. (4). This leads to $v=0$. Then, we substitute v in Eq. (3) and we get

$$u_o = \cos^{-1}\left(\frac{z}{L}\right), \tag{5}$$

where $z=L\text{-}R$. To plot the profile for u_o, we use Eq. (4) to find each value of v that corresponds to ρ and then substitute these values in Eq. (3) to get z. The same method is applied in order to find the nanotip profile and the boundary profile.

For simulating the electric field, we apply a boundary condition as follows: for the tip profile, we use the actual applied voltage, whereas the voltage at the 200 nm boundary is calculated using the following equation [39]:

$$V(u) = Vo\left(\frac{\ln\left(\tan\frac{u}{2}\right)}{\ln\left(\tan\frac{u_o}{2}\right)}\right). \tag{6}$$

The height of the nanotip is adjusted on the base profile in order to get the threshold field (5 V/Å), as illustrated in Figure 7.

We have applied this approach on different nanotips during the field evaporation of the tip atomic layers for the SAT fabricated in Figure 3. Figure 8 shows FIM images of the tip during the field evaporation process, and their corresponding FES model at each stage. The FIM images were imaged at 2.7, 3.2, 3.9, and 8.8 kV, respectively. The ring here is disconnected and has no role in the evaporation process. The model shows the overall tip profile as it gets smaller during the destruction. Figure 8D shows the base only as the nanotip is completely destructed at this stage.

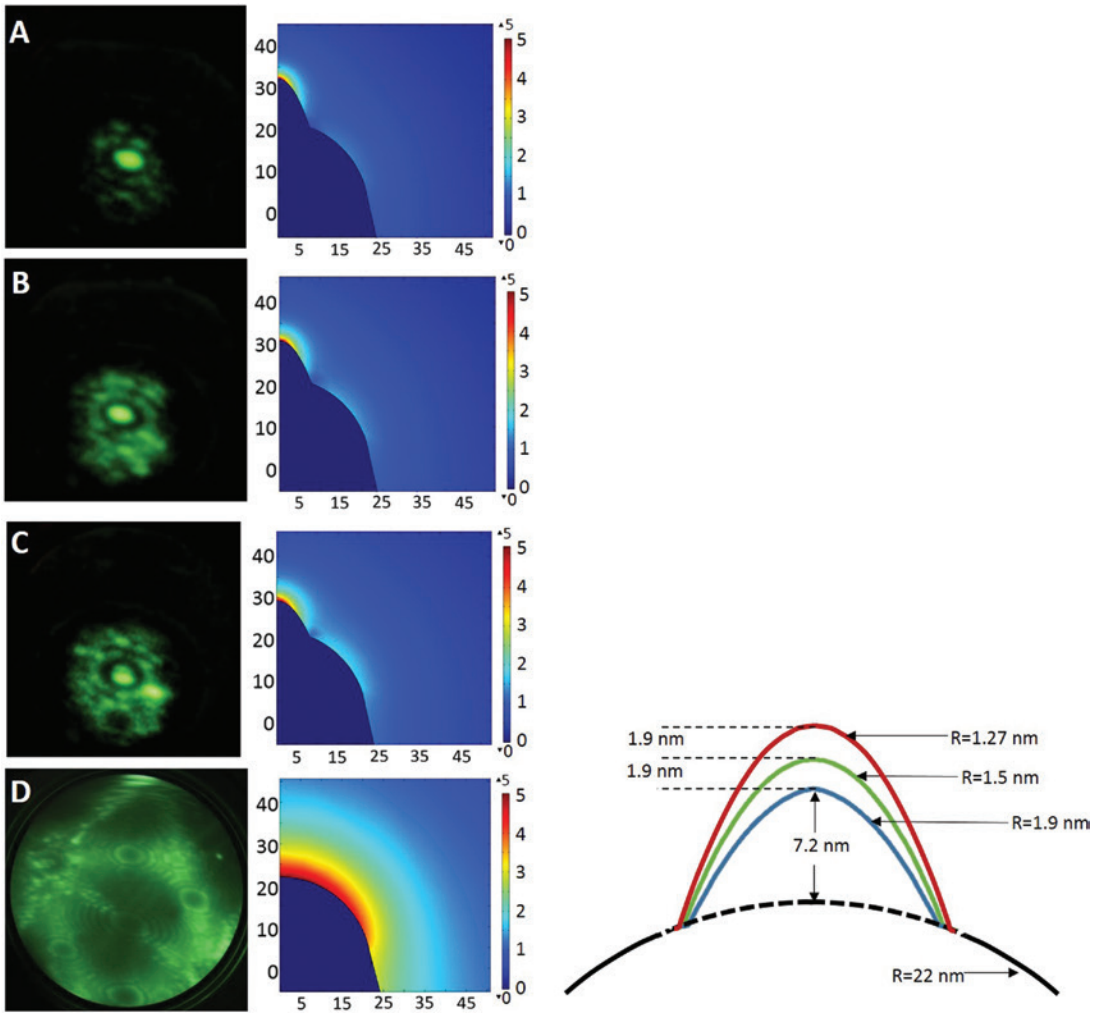

Figure 8: (A–D) FIM image sequence during the nanotip destruction process. An FES model is shown for each FIM image.

The profile plots next to the FIM images in Figure 8 show the FES models at different stages, which show the evolution of the tip shape until the entire nanotip is removed and reaches the tip base. The FES models for the nanotips in Figure 8A–C show around a 3 nm reduction in height, which is equivalent to around 13 atomic steps.

5 Conclusion

The local electron bombardment method is a new approach for fabricating ultra-sharp tips and SATs. This clean method has avoided the limitations of the previous methods and can tangibly improve the techniques of nanotip fabrication. Creating ball models is useful for estimating the nanotip apex size, especially for ultra-sharp tips (nominally <3 nm in radius) where the ring counting method does not give an accurate estimation to such tip radii. Both the nanotip apex and the tip base size significantly affect the amount of produced electric field. Therefore, we have utilized the FES analysis to use this effect to simulate the overall nanotip profile based on the applied voltage required to create the same threshold field on the base and the nanotip.

References

[1] Muller E, Tsong T. *Field Ion Microscopy: Principles and Applications*, American Elsevier Pub. Co.: New York, 1969.

[2] Miller MK, Cerezo A, Hetherington M, Smith G. *Atom Probe Field Ion Microscopy*, Clarendon Press: Oxford, 1996.

[3] Gault B, Moody MP, Cairney JM, Ringer SP. *Atom Probe Microscopy*, vol. 160, Springer Science & Business Media: Berlin, 2012.

[4] Tsong TT. *Atom-Probe Field Ion Microscopy: Field Ion Emission, and Surfaces and Interfaces at Atomic Resolution*, Cambridge University Press: Cambridge, NY, 2005.

[5] Fursey GN. *Field Emission in Vacuum Microelectronics*, Springer Science & Business Media: Berlin, 2007.

[6] Rezeq M, Joachim, C. *Nanotip Technology for Scanning Probe Microscopy*, World Scientific Publishing Co.: Singapore, 2011.

[7] Rezeq M, Ali AE, Homouz D. *Numerical and Finite Element Simulations of Nanotips for FIM/FEM*, Springer: Berlin, 2015.

[8] Binh VT, Garcia N. Atomic metallic ion emission, field surface melting and scanning tunneling microscopy tips. *J. Phys. I* 1991, 1, 605–612.

[9] Binh VT, Garcia N, Purcell S. Electron field emission from atom-sources: fabrication, properties, and applications of nanotips. *Adv. Imaging Electron Phys.* 1996, 95, 63–153.

[10] Binh VT. *In situ* fabrication and regeneration of microtips for scanning tunnelling microscopy. *Month. Microsc. J.* 2011, 3, 355–361.

[11] Binh VT, Marien J. Characterization of microtips for scanning tunneling microscopy. *Surf. Sci.* 1988, 202, L539–L549.

[12] Binh VT, Purcell S, Semet V, Feschet F. Nanotips and nanomagnetism. *Appl. Surf. Sci.* 1998, 130, 803–814.

[13] Fink HW. Mono-atomic tips for scanning tunneling microscopy. *IBM J. Res. Dev.* 1930, 86, 460–465.

[14] Song KJ, Demmin RA, Dong C, Garfunkel E, Madey TE. Faceting induced by an ultrathin metal film: Pt on W (111). *Surf. Sci.* 1990, 227, L79–L85.

[15] Szczepkowicz A, Ciszewski A. Faceting of curved tungsten surface induced by palladium. *Surf. Sci.* 2002, 515, 441–452.

[16] Niewieczerzał D, Oleksy C. Simulation of adsorbate-induced faceting on curved surfaces. *Surf. Sci.* 2006, 600, 56–65.

[17] Szczepkowicz A, Ciszewski A, Bryl R, Oleksy C, Nien C-H, Wu Q, Madey TE. A comparison of adsorbate-induced faceting on flat and curved crystal surfaces. *Surf. Sci.* 2005, 599, 55–68.

[18] Fu T-Y, Cheng L-C, Nien C-H, Tsong TT. Method of creating a Pd-covered single-atom sharp W pyramidal tip: mechanism and energetics of its formation. *Phys. Rev. B* 2001, 64, 113401.

[19] Hwang I-S, Kuo H-S, Chang C-C, Tsong T. Noble-metal covered W (111) single-atom electron sources. *J. Electrochem. Soc.* 2010, 157, P7–P12.

[20] Kuo H-S, Hwang I-S, Fu T-Y, Lin Y-C, Chang C-C, Tsong TT. Preparation of single-atom tips and their field emission behaviors. *e-J. Surf. Sci. Nanotechnol.* 2006, 4, 233–238.

[21] Chang C-C, Kuo H-S, Hwang S, Tsong TT. A fully coherent electron beam from a noble-metal covered W (111) single-atom emitter. *Nanotechnology* 2009, 20, 115401.

[22] Kuo HS, Hwang S, Fu TY, Hwang YS, Lu YH, Lin CY, Hou JL, Tsong TT. A single-atom sharp iridium tip as an emitter of gas field ion sources. *Nanotechnology* 2009, 20, 335701.

[23] Kuo HS, Hwang IS, Fu TY, Wu JY, Chang CC, Tsong TT. Preparation and characterization of single-atom tips. *Nano Lett.* 2004, 4, 2379–2382.

[24] Rezeq M, Pitters J, Wolkow R. Tungsten nanotip fabrication by spatially controlled field-assisted reaction with nitrogen. *J. Chem. Phys.* 2006, 124, 204716.

[25] Rezeq M, Pitters J, Wolkow R. A well defined electron beam source produced by the controlled field assisted etching of metal tips to <1 nm radius. *J. Scanning Probe Microsc.* 2007, 2, 1–4.

[26] Rezeq M, Joachim C, Chandrasekhar N. Confinement of the field electron emission to atomic sites on ultra sharp tips. *Surf. Sci.* 2009, 603, 697–702.

[27] Rezeq M, Joachim C, Chandrasekhar N. Nanotip apex modification with atomic precision and single atom tips restoration. *Microelectr. Eng.* 2009, 86, 996–998.

[28] Rezeq M, Ali A, Barada H. Fabrication of nano ion–electron sources and nano-probes by local electron bombardment. *Appl. Surf. Sci.* 2015, 333, 104–109.

[29] Oliva A, Romero A, Peña J, Anguiano E, Aguilar M. Electrochemical preparation of tungsten tips for a scanning tunneling microscope. *Rev. Sci. Instrum.* 1996, 67, 1917–1921.

[30] Chang W-T, Hwang S, Chang M-T, Lin C-Y, Hsu W-H, Hou J-L. Method of electrochemical etching of tungsten tips with controllable profiles. *Rev. Sci. Instrum.* 2012, 83, 083704.

[31] Hagedorn T, El Ouali M, Paul W, Oliver D, Miyahara Y, Grütter P. Refined tip preparation by electrochemical etching and ultrahigh vacuum treatment to obtain atomically sharp tips for

scanning tunneling microscope and atomic force microscope. *Rev. Sci. Instrum.* 2011, 82, 113903.
[32] Kim Y-C, Seidman DN. An electrochemical etching procedure for fabricating scanning tunneling microscopy and atom-probe field-ion microscopy tips. *Metals Mater. Int.* 2003, 9, 399–404.
[33] Fotino M. Tip sharpening by normal and reverse electrochemical etching. *Rev. Sci. Instrum.* 1993, 64, 159–167.
[34] Lucier A-S, Mortensen H, Sun Y, Grütter P. Determination of the atomic structure of scanning probe microscopy tungsten tips by field ion microscopy. *Phys. Rev. B* 2005, 72, 235420.
[35] Oliver D, Paul W, El Ouali M, Hagedorn T, Miyahara Y, Qi Y, Grütter P. One-to-one spatially matched experiment and atomistic simulations of nanometre-scale indentation. *Nanotechnology* 2014, 25, 025701.
[36] Fraser KJ, Boland JJ. Modelling of atomic imaging and evaporation in the field ion microscope. *J. Sensors* 2012, 2012, 8 pages.
[37] Rezeq M. Quantitative analysis to the electric field generated at a nano-tip and the effect of the tip base. In *GCC Conference and Exhibition (GCC), 2011 IEEE*. Piscataway, NJ: IEEE, 2011, pp. 25–28.
[38] Rezeq M. Nanotips with a single atom end as ideal sources of electron and ion beams: modeling of the nanotip shape. *Microelectr. Eng.* 2013, 102, 2–5.
[39] Rezeq M. Finite element simulation and analytical analysis for nano field emission sources that terminate with a single atom: a new perspective on nanotips. *Appl. Surf. Sci.* 2011, 258, 1750–1755.

Bionotes

Ahmed Ali
Department of Electrical and Computer Engineering, Khalifa University of Science, Technology and Research, Abu Dhabi, United Arab Emirates,
ahmed.ali@kustar.ac.ae

Ahmed Ali is a graduate student at Khalifa University, UAE. His research interest is mainly focused on experiments in the field ion microscope and the field emission microscope, such as fabrication and characterization of nanotips, which are used as probes, electron sources, and ion sources. Ahmed obtained his BSc degree in electrical and electronics engineering from the University of Sharjah in 2005.

Hassan Barada
Department of Electrical and Computer Engineering, Khalifa University of Science, Technology and Research, Abu Dhabi, United Arab Emirates

Hassan Barada is a Professor and Associate Dean of engineering at Khalifa University, UAE. He received his PhD in electrical engineering from Louisiana State University, USA, in 1989 and held various academic posts at Lehigh University (USA), King Fahd University of Petroleum and Minerals (KSA), and Etisalat University College (UAE) prior to joining KU in 2008. He has taught, published, and supervised students in areas such as distributed and parallel processing, computer architecture, and algorithm optimizations. He is a senior member of the Institute of Electrical and Electronics Engineers.

Moh'd Rezeq
Department of Electrical and Computer Engineering, Khalifa University of Science, Technology and Research, Abu Dhabi, United Arab Emirates; Department of Applied Mathematics and Sciences, Khalifa University of Science, Technology and Research, Abu Dhabi, United Arab Emirates

Moh'd Rezeq is an Associate Professor at Khalifa University of Science, Technology and Research, Abu Dhabi, UAE. Before joining Khalifa University, Dr. Rezeq worked in a few nanotechnology laboratories in Singapore and Canada. His research interests cover some areas like semiconductor-based nano-electronic devices, scanning probe microscopy, nano-probes: fabrication and characterization, nano-materials characterization, and field ion and electron microscopy. He has supervised several graduate and undergraduate students in nanotechnology fields.